Proceedings of the 21st ICSMGE, Vienna, Austria, 14 – 19 June 2026. Pistrol, Adam & Schweiger (eds.)
Published by: ÖGG, Austrian Society for Geomechanics, Salzburg, Austria, ISBN 978-3-9503898-4-5
https://doi.org/10.53243/ICSMGE2026-1146

Micromechanical Investigation of Intergranular Strain Concept in Hypoplastic Models Through DEM Simulations

Mohammad Salimi, Merita Tafili, Nazanin Irani, and Torsten Wichtmann
Ruhr University Bochum, Chair of Soil Mechanics, Foundation Engineering and Environmental Geotechnics, Faculty of Civil and Environmental Engineering, 44801 Bochum, Germany, mohammad.salimi@rub.de

ABSTRACT: Hypoplastic models exhibit well-known limitations under cyclic loading, particularly in modeling small hysteretic loops and in avoiding excessive strain accumulation during stress cycles. To mitigate these shortcomings, the concept of intergranular strain, $\boldsymbol{h}$, was introduced as an additional tensorial state variable representing the deformation of a particle-scale interface layer and capturing recent deformation history. Although this extension has been successfully applied in various hypoplastic models for clay and sand, its phenomenological character remains a point of criticism. In this study, discrete element method (DEM) simulations are utilized to quantify the second-order work and to provide a micromechanical basis for the intergranular strain concept. A comprehensive series of DEM simulations, including drained, undrained triaxial loading as well as true triaxial paths with unloading-reloading cycles, were performed to analyse the evolution of stiffness during stress and strain reversals. The micromechanical evaluation of the second-order work demonstrates that this framework effectively explains the role and behaviour of intergranular strain from a micromechanical perspective.

KEYWORDS: Discrete Element Method (DEM); hypoplastic model; Intergranular strain; Granular materials.

1 INTRODUCTION

Constitutive models are fundamental tools in geotechnical engineering, enabling the prediction of soil behavior under diverse loading conditions and informing the safe design of civil infrastructure. Among the available frameworks, elasto-plastic and hypoplastic formulations have been widely adopted, each offering distinct advantages in capturing the nonlinearity and path dependency of granular materials.

In elasto-plastic models, changes in loading direction—such as those occurring during unloading-reloading or cyclic processes—are often addressed through kinematic hardening or bounding surface concepts. By explicitly coupling elastic and plastic responses, these models can represent stiffness recovery and degradation during load reversals, making them well suited for cyclic and repeated loading scenarios. They require the definition of a yield surface separating elastic and plastic regimes, often complemented by state-dependent dilatancy rules to account for stress–density effects. Despite their theoretical capabilities, these models rely on the assumption of a clearly identifiable elastic domain, the size and shape of which can vary considerably between formulations and experimental interpretations. Laboratory studies suggest that this domain may be significantly smaller than assumed, and that the transition from recoverable to irrecoverable strain may be gradual rather than sharply delineated, challenging one of the fundamental assumptions of classical elasto-plasticity.

Hypoplasticity, introduced by Kolymbas (1977) as an incrementally nonlinear framework tailored to granular materials, eliminates the explicit separation between elastic and plastic strains and can describe a wide range of monotonic and non-monotonic loading paths. However, the original formulation is unable to reproduce small-strain cyclic behavior and typically leads to unrealistic ratcheting under very small load cycles. To address this, Niemunis and Herle (1997) introduced the intergranular strain concept, a history-dependent state variable representing the deformation of a particle-scale interface layer. This modification substantially improved the ability of hypoplasticity to reproduce small cyclic loops and has since been successfully incorporated into hypoplastic models for both sands and clays. Nevertheless, the concept remains phenomenological, and its direct correlation to measurable microstructural features has yet to be conclusively established.

Despite considerable advances in both modelling categories, neither offers a fully satisfactory representation of stiffness evolution during load reversals or cyclic loading. Experimental observations (Wood, 2004) and DEM simulations (e.g., Lu et al., 2025; Pouragha, 2022) indicate that the separation between “elastic” and “plastic” parts of deformation is less clear-cut than most constitutive frameworks assume, and additional criteria are typically required to enforce this partition. DEM (Cundall, 1997) provides a valuable perspective on probing the micro-mechanical origins of stiffness change without imposing such predefined separations.

In this study, we examine the original hypoplastic model of von Wolffersdorff (1996) in combination with three intergranular strain (IGS) formulations: Niemunis and Herle (1997), Fuentes and Triantafyllidis (2015), and Mugele et al. (2024); and employ DEM simulations to investigate the micromechanical foundations of the IGS concept. By quantifying variables such as the second-order work and linking them to model assumptions, we aim to identify potential refinements to the intergranular strain concept, with the broader goal of informing constitutive modeling strategies that more accurately reflect the observed soil response.

2 THEORY

In this section, the parameters that serve as a link between the assumptions in hypoplasticity and their physical interpretation based on DEM simulations are described.

2.1 *Micro-Scale Analysis in DEM*

An effort to connect the macroscopic behavior of granular materials with their underlying microstructure was made by Nicot et al. (2014), aiming to provide a deeper understanding of failure mechanisms in granular assemblies. To this end, key microstructural mechanisms that are most likely to trigger the nucleation and propagation of instabilities were investigated. Central to this analysis is the concept of second-order work, which serves as a predictive variable for the onset of failure and can be expressed in terms of grain-scale quantities. Although the intergranular strain exerts an opposing influence on failure initiation, the second-order work formulation proposed by Nicot et al. (2014) remains a useful framework for exploration.

At the macroscopic level, the stress within a representative volume V can be expressed using the Eulerian Love-Weber formula:

$$\sigma_{ij} = \frac{1}{V}\sum_{c=1}^{N_c} f_i^c l_j^c + \frac{1}{V}\sum_{p\in V} f_i^p x_j^p \quad (1)$$

where l^c is the branch vector of contacting particles at contact c, f^c is the corresponding contact force, f^p is the resultant external force applied to particle p, and x^p denotes the particle's position.

At the micro-mechanical level, the second-order work is expressed as:

$$d^2W = \sum_{p,q} \delta f_i^c \delta l_i^c + \sum_{p\in V} \delta f_i^p \delta x_i^p \quad (2)$$

Here, the first term captures the intricate coupling between the contact force network (f^c) and the geometrical distribution of branch vectors (l^c), while the second term accounts for the contribution of incremental unbalanced forces on individual particles. The latter term is often negligible when inertial effects are small, but it can become significant in the plastic regime, where particle rearrangements (e.g., sliding, contact creation, and contact opening) lead to a reduction of the overall soil stiffness.

The inter-particle contact fabric tensor $\boldsymbol{F}$ is defined as:

$$\boldsymbol{F} = \frac{1}{2N_c}\sum_{k=1}^{2N_c} n_c^k \otimes n_c^k \quad (3)$$

where N_c is the total number of inter-particle contacts. In this expression, $\boldsymbol{F}$ denotes the direction cosines of the *k*-th unit contact normal vector with respect to the reference axes x_i ($i \in \{1,2,3\}$). The factor of 2 in the summation compensates for the double-counting of contacts and ensures the symmetry of the resulting fabric tensor.

The degree of fabric anisotropy is quantified using scalar parameters, such as Δ, which is derived from the deviatoric components of the respective fabric tensor:

$$\Delta = \sqrt{3(\boldsymbol{F}^*:\boldsymbol{F}^*)} \quad (4)$$

where F^* is the deviatoric part of F.

2.2 *Intergranular Strain (IGS)*

In the context of intergranular strain, $\boldsymbol{h}$, is introduced to account for transient modifications of soil stiffness following changes in strain path direction. The maximum magnitude of $\boldsymbol{h}$ is treated as a material constant, *R*, assumed to be independent of pressure or void ratio.

Intergranular Strain (IGS) – Niemunis & Herle (1997)

The original intergranular strain concept by Niemunis & Herle (1997) was introduced to address the shortcomings of classical hypoplastic models in reproducing small-strain behavior, particularly to reduce the excessive accumulation of strain (ratcheting) under cyclic loading. The new tensorial state variable, $\boldsymbol{h}$, evolves within a constant-size small-strain domain, independent of stress level, and allows for a sudden stiffness increase upon load reversal and a gradual stiffness reduction during monotonic straining. By coupling this mechanism to the hypoplastic stress–strain law, the model captures small-strain stiffness, path-dependence, and the memory effect of recent strain history, while retaining hypoplasticity's ability to model large-strain behavior without explicit elastic–plastic decomposition.

Intergranular Strain Anisotropy (ISA) – Fuentes & Triantafyllidis (2015)

The ISA model extends the IGS concept by introducing a yield surface in the intergranular strain space, defined as a hypersphere centered on a back-intergranular strain variable. This innovation enables the explicit modeling of memory effects and stiffness recovery upon reversal loading while reducing stiffness overshooting problems seen in earlier IGS implementations. The model incorporates a hardening law for the back-intergranular strain, inspired by bounding surface plasticity, and links plastic flow in the mechanical stress–strain relation directly to the plastic evolution in the intergranular strain space. For medium and large strain amplitudes, the formulation reduces to a form equivalent to classical Karlsruhe hypoplasticity, while for small strains it reproduces key effects such as stiffness increase, plastic strain reduction during unloading, and cyclic hysteresis.

Generalized Intergranular Strain (GIS) – Mugele et al. (2024)

The GIS framework generalizes the intergranular strain so it can be applied to a wide range of constitutive models, including both hypoplastic and elasto-plastic formulations. Building on the IGS and its improved variant (ISI proposed by Duque et al., 2020), GIS introduces a flexible mapping between the base model's state variables and the intergranular strain evolution, ensuring compatibility with formulations that incorporate an asymptotic state boundary surface. It addresses limitations of earlier IGS-types, notably overshooting, difficulty in transferring the concept to other models, and limited accumulation modeling. In essence, GIS preserves the small-strain benefits of IGS/ISA, avoids their numerical drawbacks, and provides a base-model-independent, extensible small-strain enhancement layer for advanced soil constitutive modeling.

To provide a general mathematical representation of the intergranular strain concept applicable to all three formulations (IGS, ISA, and GIS), the evolution of the intergranular strain tensor $\boldsymbol{h}$ from the ISA formulation can be expressed in a unified form as:

$$\dot{\boldsymbol{h}} = \dot{\boldsymbol{\varepsilon}} - \lambda_h \boldsymbol{N} \quad (5)$$

where $\dot{\boldsymbol{\varepsilon}}$ is the total strain rate tensor, $\boldsymbol{N} = (\boldsymbol{h} - \boldsymbol{c})/\|\boldsymbol{h} - \boldsymbol{c}\|$ is the unit normal to the intergranular strain yield surface in the intergranular strain space, and $\mathbf{c}$ denotes the back-intergranular strain tensor (which vanishes for the original IGS and GIS model). The scalar λ_h governs the inelastic evolution in the intergranular strain space and is defined through a model-specific function

$$\lambda_h = \varphi(\boldsymbol{h}, \dot{\boldsymbol{\varepsilon}}, \boldsymbol{\alpha}) \quad (6)$$

with $\boldsymbol{\alpha}$ representing any additional state variables, such as the historiotropic scalar introduced in GIS to capture cyclic accumulation effects.

This formulation highlights the common framework behind the different models: all describe the progression of $\boldsymbol{h}$ as the sum of the applied strain rate and a corrective term proportional to the loading direction in intergranular strain space. φ is chosen to limit $\|\boldsymbol{h}\|$ within a constant elastic range of the magnitude R, reproducing stiffness increase upon reversal and gradual stiffness degradation during monotonic loading.

By presenting the intergranular strain evolution in this compact form, the small-strain enhancement mechanisms of IGS, ISA, and GIS can be seen as specific cases of a single theoretical framework, differing only in the definition of φ and the presence or absence of back-intergranular strain and extra state variables. This unified view facilitates both conceptual understanding and implementation into a variety of hypoplastic and elasto-plastic formulations. Since the key parameter controlling the change in stiffness due to unloading in hypoplasticity with small-strain effects is the intergranular strain $\boldsymbol{h}$, it is of particular interest to relate this macroscopic state variable to micro-scale information obtained from DEM. In the following, we perform DEM simulations of loading–unloading cycles and extract quantities that can be directly linked to the evolution of $\boldsymbol{h}$ in all three approaches: IGS, ISA and GIS.

From a micromechanical standpoint, $\boldsymbol{h}$ characterizes the average elastic-type deformation of the contact network before irreversible rearrangements of the grain skeleton occur. In DEM simulations, this can be evaluated through changes in branch vectors within the contact network. During unloading, $\boldsymbol{h}$ increases as the contact network recovers, until the maximum range of the intergranular strain domain is reached, beyond which sliding and contact rearrangements reinitiate. As will be shown in the following sections, DEM results provide direct explanation of $\boldsymbol{h}$ and its evolution, revealing some discrepancies with the predictions of existing IGS, ISA, and GIS formulations. These differences highlight the need to refine the intergranular strain concept to better capture the true micromechanical behavior observed in DEM, and to more accurately link micro-scale contact mechanics with the macroscopic stiffness changes in hypoplastic models.

3 RESULTS AND DISCUSSION

A comprehensive series of DEM simulations was performed on a granular assembly consisting of 10,000 spherical particles subjected to drained triaxial loading–unloading conditions. The initial relative density D_{r0} was varied at three levels. 33 %, 62 %, and 110 %, while the initial mean effective pressure was kept constant at 100 kPa. Cyclic perturbations were applied systematically: unloading–reloading loops were introduced at every 5 % increment of shear strain, and their amplitudes were prescribed to remain constant, progressively decrease, or progressively increase. In the program presented herein, the focus is placed on controlled cyclic perturbations with progressively decreasing amplitude, corresponding to 90 %, 50 %, and 5 % of the shear stress mobilized at the respective strain level. The evolution of contact-network anisotropy was quantified through the fabric tensor and its scalar invariant Δ.

In parallel, additional monotonic DEM triaxial tests were used to calibrate the three hypoplastic models examined in this study (IGS, ISA, and GIS). The calibrated models were then employed to compute the perturbation simulations and evaluate the evolution of the Frobenius norm of the intergranular strain, $\|\boldsymbol{h}\|$. This quantity was directly compared to the micro-scale second-order work d^2w obtained from DEM. The choice of d^2w is motivated by its micromechanical completeness: whereas the intergranular strain in hypoplasticity reflects changes in the "strain state'' of the contact network, the second-order work intrinsically accounts for the evolution of both branch vectors and contact forces. This makes it a suitable benchmark for assessing, and potentially refining, the intergranular strain concept.

Figure 1 shows the macroscopic shear stress (q) versus shear strain (ε_q) response from DEM alongside the predictions of the hypoplastic (Hypo) model coupled with IGS, ISA, and GIS models, demonstrating that all three reproduce the overall mechanical behavior under the considered loading-unloading-reloading scenarios.

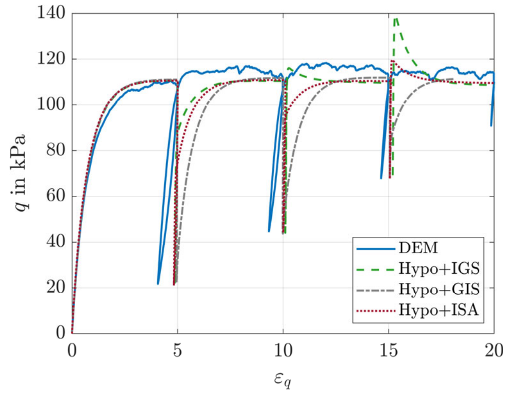

Figure 1: Macroscopic shear stress–shear strain response from DEM loading–unloading–reloading simulations, compared with predictions of Hypo+IGS, Hypo+ISA, and Hypo+GIS models.

Figure 2(a) presents the evolution of $\|\boldsymbol{h}\|$, predicted by the three hypoplastic models, while Figure 2(b) shows the corresponding micro-scale second-order work obtained from DEM. The comparison reveals several important trends. In all unloading–reloading scenarios, the three hypoplastic models predict almost identical changes in $\|\boldsymbol{h}\|$ reaching the same maximum magnitude during unloading. The main difference between the models lies in the rate at which $\|\boldsymbol{h}\|$ returns toward its initial value during subsequent reloading. This indicates that, within the current formulations, the amplitude of unloading primarily affects the recovery rate rather than the peak change in $\|\boldsymbol{h}\|$. Furthermore, the predicted $\|\boldsymbol{h}\|$ evolution is essentially independent of the shear strain level at which unloading occurs.

By contrast, the DEM-derived second-order work, d^2w, exhibits a different behavior. The magnitude and shape of the d^2w response vary significantly with the shear strain at which unloading takes place. Specifically, for a given unloading amplitude, the change in micro-scale second-order work is larger when unloading occurs at a higher ε_q. This implies that the amplitude of unloading is not the dominant factor governing micro-scale energy changes; rather, the strain state of the sample at the moment of unloading plays a more important role. A plausible explanation is that, with increasing shear strain, a greater fraction of particles becomes mobilized and aligned with the loading direction, leading to a more anisotropic contact network. Reversing or altering the load direction in such a configuration requires more energy—manifested as a higher stiffness—to overcome the established microstructural alignment.

An interesting point is that, in reloading phases where the soil does not undergo large strain reversals, the DEM still shows an elevated stiffness response. This can be understood by considering that the energy invested in reorienting particles during the initial reversal must be spent again for subsequent directional changes. As a result, unloading–reloading cycles tend to produce d^2w values of similar magnitude, with the primary difference appearing in the rate at which the response decays toward zero. These micro-mechanical observations suggest that the current mathematical representation of $\|\boldsymbol{h}\|$ in hypoplasticity does not fully capture the strain-history-dependent anisotropic stiffening revealed by DEM, underscoring the need for refinement of the intergranular strain concept, particularly for scenarios involving multiple loading cycles.

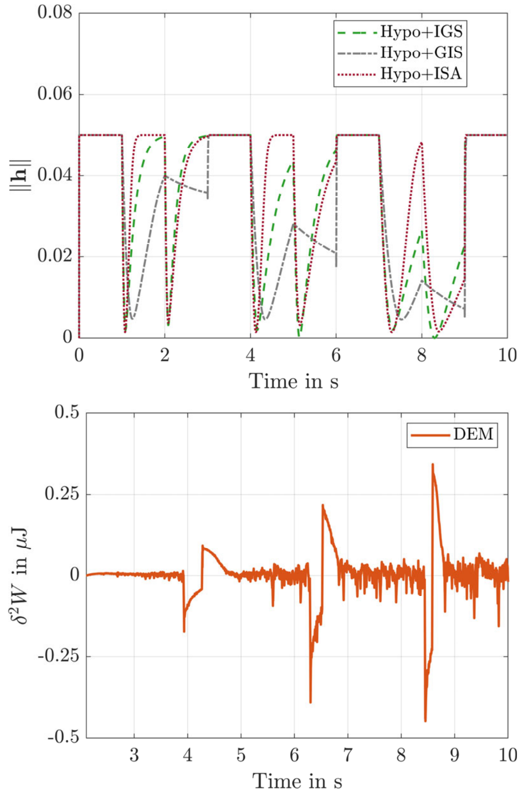

Figure 2. (a) Evolution of the Frobenius norm of the intergranular strain, $||\boldsymbol{h}||$, predicted by Hypo+IGS, Hypo+ISA, and Hypo+GIS models under loading–unloading–reloading conditions. (b) Corresponding micro-scale second-order work from DEM simulations, capturing both branch vector changes and contact force evolution.

Figure 3 shows the evolution of the fabric tensor components and its invariant under various loading–unloading–reloading paths. While fabric changes with loading history, these variations do not align with the stiffness trends from DEM second-order work. This indicates that contact fabric alone cannot explain stiffness recovery, and the intergranular strain concept likely requires additional microstructural descriptors beyond fabric anisotropy.

4 CONCLUSIONS

The present DEM simulations on granular assemblies under various loading–unloading–reloading scenarios were used to evaluate three hypoplastic models with intergranular strain enhancements (IGS, ISA, and GIS) and to compare their predictions of the Frobenius norm of the intergranular strain, $||\boldsymbol{h}||$, with DEM-derived micro-scale second-order work. While all models reproduced the macroscopic stress–strain response and predicted similar magnitudes of $||\boldsymbol{h}||$ changes, they do not capture the pronounced dependence of micro-scale stiffness changes on the shear strain level at which unloading occurred. DEM results showed that unloading amplitude had limited influence compared to strain history, with higher strains producing greater second-order work peaks due to increased particle alignment and contact network anisotropy.

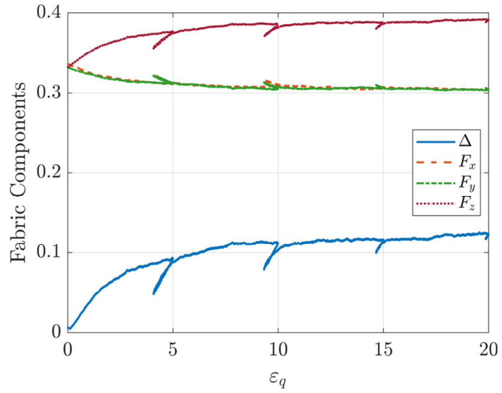

Figure 3. Evolution of the fabric tensor components and the fabric invariant, Δ, versus shear strain for different loading–unloading–reloading scenarios in DEM simulations.

5 REFERENCES

Cundall, P. A., & Strack, O. D. L. (1979). A discrete numerical model for granular assemblies. Geotechnique, 29(1), 47–65. https://doi.org/10.1680/geot.1979.29.1.47

Duque, J., Mašín, D., & Fuentes, W. (2020). Improvement to the intergranular strain model for larger numbers of repetitive cycles. Acta Geotechnica, 15(12), 3593-3604.

Fuentes, W., & Triantafyllidis, T. (2015). ISA model: A constitutive model for soils with yield surface in the intergranular strain space. International Journal for Numerical and Analytical Methods in Geomechanics, 39(8), 775–796. https://doi.org/10.1002/nag.2370

Icot, F., Hadda, N., Sibille, L., Radjai, F., Hicher, P.-Y., & Darve, F. (2014). Some micromechanical aspects of failure in granular materials based on second-order work. Comptes Rendus Mécanique, 342(3), 174–188. https://doi.org/10.1016/j.crme.2013.12.006

Kolymbas, D., & Herle, I. (1998). Hypoplasticity: A framework to model granular materials. In Behaviour of granular materials (pp. 239–268). Springer. https://doi.org/10.1007/978-3-7091-2674-4_9

Lu, D., Jin, H., Gao, Z., Zhou, X., & Du, X. (2024). Stress probing investigation of the yield and plastic flow of sand. Geotechnique, 1–12. https://doi.org/10.1680/jgeot.24.01222

Mugele, L., Stutz, H. H., & Mašín, D. (2024). Generalized intergranular strain concept and its application to hypoplastic models. Computers and Geotechnics, 173, 106480. https://doi.org/10.1016/j.compgeo.2023.106480

Muir Wood, D. (2004). Experimental inspiration for kinematic hardening soil models. Journal of Engineering Mechanics, 130(6), 656–664. https://doi.org/10.1061/(ASCE)0733-9399(2004)130:6(656)

Niemunis, A., & Herle, I. (1999). A model for the behaviour of soils under cyclic loading. International Journal for Numerical and Analytical Methods in Geomechanics, 23(8), 629–652. https://doi.org/10.1002/(SICI)1096-9853(19990610)23:8<629::AID-NAG960>3.0.CO;2-#

Niemunis, A., Wichtmann, T., & Triantafyllidis, T. (2011). Hypoplastic model with elastic strain range. Computers and Geotechnics, 38(7), 833–843. https://doi.org/10.1016/j.compgeo.2011.05.002

Pouragha, M., Eghbalian, M., & Wan, R. (2020). Micromechanical correlation between elasticity and strength characteristics of anisotropic rocks. International Journal of Rock Mechanics and Mining Sciences, 125, 104154. https://doi.org/10.1016/j.ijrmms.2019.104154

Von Wolffersdorff, P. A. (1996). A hypoplastic relation for granular materials with a predefined limit state surface. Mechanics of Cohesive-frictional Materials: An International Journal on Experiments, Modelling and Computation of Materials and Structures, 1(3), 251-271.

Wiebicke, M., Herle, I., Andò, E., & Viggiani, G. (2021). Measuring the fabric evolution of sand: Application and challenges. Geotechnik, 44(2), 114–122. https://doi.org/10.1002/gete.202000019